Deforestation Detection in Indonesian Tropical Forest Using Multi-Temporal ALOS/PALSAR Backscatter Data

I GD Yudha Partama[1], *Tasuku* Tanaka[2], *Kakuji* Ogawara[2], *Takahiro* Osawa[3], *Putu* Sujana[1]

[1]Postgraduate Program on Regional Planning and Environmental Management, Mahasaraswati University,Denpasar, Indonesia
[2]Graduate School of Science and Engineering, Yamaguchi University, Yamaguchi, Japan
[3]Center for Remote Sensing and Ocean Science (CReSOS), Udayana University

Abstract. This study tested the effectiveness of multi-temporal Phased Array L-band Synthetic Aperture Radar (PALSAR) data to detect the deforestation in tropical forest region, Riau Province, Indonesia. The image differencing method by using a threshold was utilized for automatic detection of deforestation mapping. In addition, the influence of SAR polarization and seasonal changing due to rainfall event on accuracy of deforestation detection was investigated. Overall, we obtained the following results: (1) the accuracy of deforestation detection mapping using horizontal transmit-vertical receives (HV) polarization is giving better results than horizontal transmit-horizontal receives (HH) polarization. (2) The seasonal changing due to rainfall event affected the radar backscattering signatures of deforested areas and deforestation detection accuracy. High-accumulated precipitation decreased the sigma nought (σ^0) difference between deforested areas and natural forests, causing decreased accuracy of deforestation detection. The best selection of PALSAR data before detection and fixing a threshold value can be one of alternative to reduce the error in automatic detection. The overall accuracy of deforestation detection mapping using a fixed threshold was 92.21%. The deforestation mapping method proposed in the study can be utilized for assessment of yearly changes in forested areas and is useful for tracking changes in forest cover on large scales.

1 Introduction

Indonesia's rainforests are among the richest in the world in terms of biodiversity, and include significant deep peat on the planet. Recently, the Indonesian rainforests have been under significant pressure due to the expansion of industrial oil-palm and pulpwood plantations, as well as increased vulnerability to fire, threatening one of the world's most bio-diverse and carbonrich forests. The Indonesian government estimates that, for each year

[1] Corresponding author: yudhapartama46@gmail.com

between 2003 and 2006, around 1.17 million ha of forest was cleared and degraded (WWF Indonesia, 2008).

Satellite remote sensing is viewed as a viable, cost-effective, and verifiable tool for monitoring the large forest cover and their changes in order to provide suitable information for the objective of the United Nations Framework Convention on Climate Change (UNFCCC) and Reducing Emission from Deforestation and Forest Degradation (REDD+) program. Optical remote sensing data is used in many studies to monitor the status of tropical forests (Hansen et al., 2008; Tsuyukiet al., 2011; Margono et al., 2012). However, optical sensor is often difficult to provide the cloud-free images in the tropical regions due to frequent cloud cover and haze from forest fire.

One of the most promising approaches for mapping deforestation with finer temporal and spatial resolution is the use of synthetic aperture radar (SAR) data. SAR technology can be used to observe the ground surface even when clouds cover the ground because of the cloud penetration capability of microwaves. Advanced Land Observing Satellite (ALOS) Phased Array L-Band Synthetic Aperture Radar (PALSAR) with long radar wavelength L-band (23.62 cm wavelength) and finer resolution (12.5 m) is better suited to the delineation of forest cover and deforestation detection on the regional and global scale because of greater penetration through canopy (Shimada, 2009).

On the other hand, the accuracy of deforestation detection using SAR images is influenced by several factors such as environmental conditions and the characteristics of SAR system (polarization and wavelength) (Kiage et al., 2005). Japanese Earth Resources Satellite-1 (JERS-1) with only using co-polarized (HH-polarization) backscatter data was found to be difficult to distinguish between natural forest and deforested areas, and affected the accuracy of deforestation detection mapping (Thiel C et al., 2006). ALOS/PALSAR data provided the Fine Beam Dual Polarization (FBD) mode with HH and HV polarization. The study to evaluate the SAR system polarization with different polarization (HH and HV polarizations) is needed to establish the robust method for deforestation detection mapping.

Another factor that can affect the accuracy of deforestation detection is the presence of environmental conditions (eg rainfall) at the time of image acquisition. The largest contrast (dynamic range) between mean forest backscatter and mean deforested backscatter appear in the driest season and the lowest contrast appear in the wet season (Salas et al., 2002; Whittle et al., 2012). Temporal and spatial variability of JERS-1 backscatter data for deforested areas was explained as a consequence of rainfall events and heterogeneous of soil moisture distribution (Salas et al., 2002). To reduce errors in the interpretation of deforestation detection, it is necessary to evaluate the stability of the thresholding method based on the effects of seasonal changes caused by rainfall events.

The objective of this study is to examine the potential of using multi-temporal ALOS PALSAR FBD data to: 1) Investigate the influence of SAR polarization on the accuracy of deforestation detection mapping; 2) Investigate the influence of seasonal changing due to rainfall event on radar backscattering signatures in tropical environment regions; 3) Set up the method for deforestation detection and calculate the accuracy of deforestation map using thresholding method; 4) Calculate the percentage of forest cover loss by thresholding method in Riau study area.

2 Methods

2.1 Study area

The research location was focused in Riau province on Sumatra Island, Indonesia which located between 2042'N -1012'S latitude and 100000'E-104000'E longitude (Figure 1). The location was chosen based on the Global Forest Watch (GFW) data that the most intense recent large-scale natural forest clearance. Recent deforestation has been caused mainly by conversion to acacia (for pulp and paper production) and oil palm plantations. Riau has tropical climate with relatively high rainfall, ranging from 2000 to 3000 mm per year with approximately 207 days of rain per year (BPS, 2009). Rainy season falls on November/October up to April while dry season begin in June/July.

Fig 1. Study Area

2.2 Data collection

Repeat ALOS/PALSAR FBD images over Riau Province consist of HH-HV polarized image pairs, with 12.5x12.5 m pixel spacing and off nadir angle is 34.30. FBD images was processed at level 1.5 (which includes radiometric correction, range and multi-look azimuth compression, geocoding and orthorectification process) from 2007-2010. These data are suitable for flat terrain area.

To evaluated the accuracy of deforestation detection mapping, yearly of gross forest cover loss event as reference dataset in deforested areas were downloaded from Global Forest Change, University of Maryland (http://earthenginepartners.appspot.com) from 2007-2010. The time-series of dataset were generated using multispectral Landsat 7 ETM+ sensor (Hansen et al., 2013). The data set measures areas of tree cover loss all global land at 30 x 30 meter resolution. Tree cover loss may indicate a number of potential activities, such as timber harvesting, fires or disease, the conversion of natural forest to other land uses, or the crop rotation cycle of tree plantations (Hansen et al., 2013).

Rainfall data from Daily Global Satellite Mapping of Precipitation (GSMap) are used to investigate the influence of seasonal change on time variations of PALSAR backscatter data. The spatial resolution of the data was 0.250 by 0.250. The daily data sets were collected during the 2007-2010 time period by downloading from the GSMap Data Archive Center. The 10-day accumulated precipitation before the PALSAR observation date for each reference point then calculated to be a possible indicator of the surface moisture condition.

2.3 Data analysis method

The research framework are divided into two parts, the research frame work 1 shows the flow chart of evaluation the influence of SAR polarizations and seasonal changing on the accuracy of deforestation detection by using thresholding method. Thresholding method used to determine the threshold value of σ^0 difference from image before and after deforestation events. To evaluated the accuracy of threshold detection, the detection rate (DR), false alarm rate, and accuracy rate (AR) at the reference point for different thresholds was calculated.

The research framework 2 shows the flow chart of evaluation the influence of seasonal changing on the radar backscattering value. In this step, Digital Number (DN) of ALOS/PALSAR FBD was converted to Normalized Radar Cross Section (NRCS) in dB unit. Then, the region of interest (ROI) for each Land Use/Land Cover (LU/LC) from NRCS images based on ground truth point from secondary data was extracted. Analysis of correlation between 10-days accumulated rainfall and NRCS was conducted to get the coefficient of determination (R^2) from the relationship.

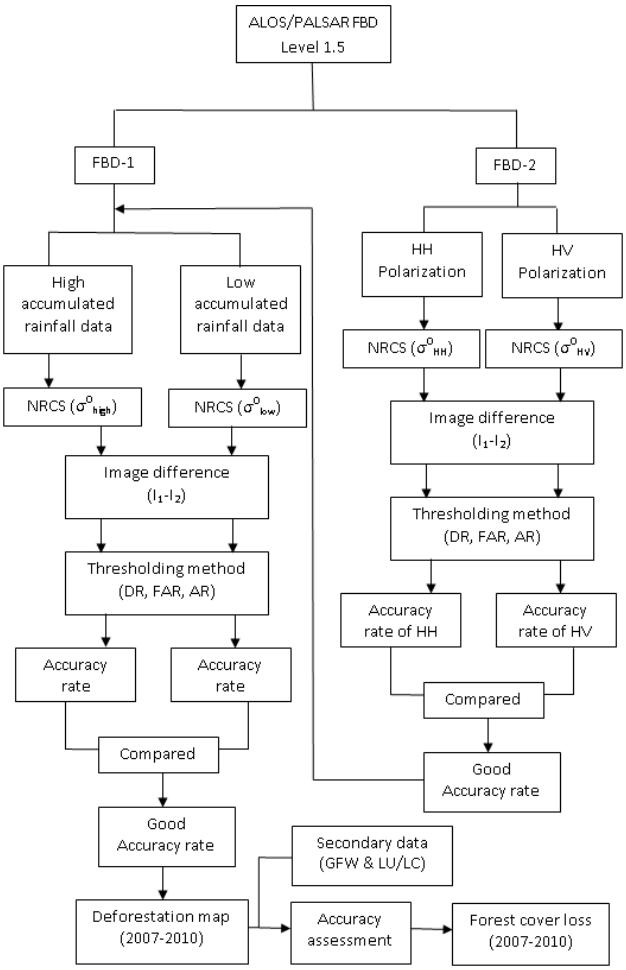

Fig 2. Research Framework 1

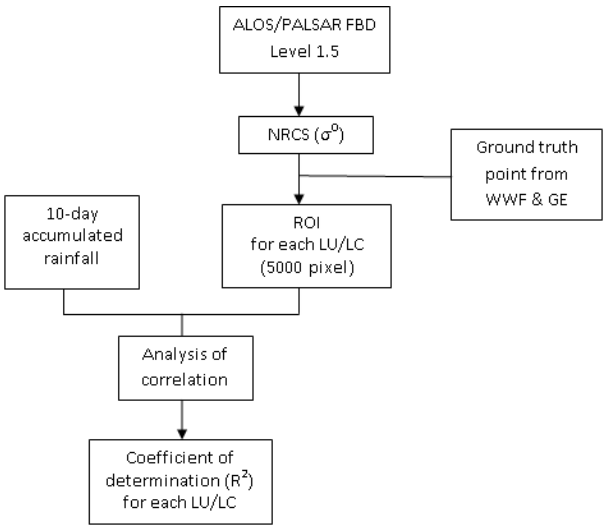

Fig 3. Research Framework 2

2.4 Data Processing

2.4.1 Pre-processing of the time series of PALSAR FBD data

The multi-temporal of PALSAR FBD 1.5 level data were filtered using Low Pass filter with a 3x3-window size to reduce the speckle and noise. The DN values were converted into NRCS in decibel (dB) unit according to the formula from JAXA and the parameters from the metadata of each file (Shimada, 2009):

$$\sigma^0 [dB] = 10 \times \log10 (DN)^2 + CF \quad \text{.....(1)}$$

Where σ^0 is the backscattering coefficient, DN is the digital number value of pixels in HH or HV polarization and CF is the absolute calibration factor of -83.

2.5 Data analysis

2.5.1 Change detection method for deforestation mapping

a. Image Differencing

In this technique, PALSAR images of the same area after converted to σ^0, obtained from time t_1 (after deforested) and t_2 (before deforested), were subtracted pixel wise. Mathematically, the difference image is

$$\sigma^0_d (x, y) = \sigma^0_1(x,y) - \sigma^0_2(x,y) \quad \text{.....(2)}$$

Where, σ^0_1 and σ^0_2 are the images obtained from t_1 and t_2, (x,y) are the coordinates of the pixels. The resulting images, σ^0_d represent the backscatter intensity difference of σ^0_1 and σ^0_2.

b. Evaluation of thresholding method for deforestation detection

The detection rate (DR), false alarm rate (FAR) and accuracy rate (AR) was calculated to evaluate the accuracy of threshold detection. The detection rate is defined as the probabilities if a pixel is detected as "deforested" by PALSAR (DF_{PALSAR}) when it is "deforested" by reference data ($DF_{reference}$). The detection rate is estimated as (Motohka et al., 2014):

$$DR = P(DF_{PALSAR}|DF_{reference}) \quad \text{.....(3)}$$

The false alarm rate is defined as the probabilities if a pixel is detected as "deforested" by PALSAR (DF_{PALSAR}) when it is "Un-disturb forest" by reference data ($UF_{reference}$). The false alarm rate estimated as

$$FAR = P(DF_{PALSAR}|UF_{reference}) \quad \text{.....(4)}$$

The accuracy rate (AR) is total correct detection (deforested area and un-disturb forest; $N_{correct}$) divided by the total number of pixels (N_{total}). The accuracy rate estimated as

$$AR = N_{correct}/N_{total} \quad \text{.....(5)}$$

2.5.2 Evaluation of HH and HV polarization to detect the deforestation

The FBD images (HH and HV) acquired in 2007 and 2009 were selected to evaluate the ability of polarization to detect the deforestation. The Region of Interest (ROIs) was selected in both of deforested and natural forest areas according to the reference data from Global Forest Watch and LU/LC. The total pixel selected is 5000 pixel for each land cover. The polarization, which has good accuracy rate, will be selected for following analysis.

2.5.3 Evaluation of seasonal variations effect on deforestation detection

The multi-temporal PALSAR FBD images from 2007-2010 were selected to evaluate the seasonal changing effect on accuracy of deforestation mapping. The FBD image acquired at 2007 are used as a standard for calculations (σ^0_2) and we selected the time series images from 2009-2010 (σ^0_1) to compare the difference in the accuracy of deforestation detection between high and low accumulated precipitation data.

2.6 Deforestation mapping

Based on the results of the above analysis, deforestation map from 2009-2010 was generated using multi-temporal ALOS/PALSAR FBD-1 data. The first step is calculating the σ^0 difference between the input and base images. Non-forest areas were masked using the forest/non-forest map. Deforestation mapping results were obtained by applying a threshold determined by the above mentioned analysis for multi-temporal σ^0 difference. The deforestation map from each year was combined to make the final deforestation map

(November 2007 to October 2010). The accuracy of deforestation map was evaluated by using confusion matrix method. The areas and percentage of deforested are calculate using Arc GIS Ver. 9.3 software.

3. Results and Discussion

3.1 Evaluation of HH and HV polarization to detect the deforestation

Figure 4 shows the characteristic of backscatter value (σ^0) for HH and HV polarization during the deforestation event. Based on this Figure, the temporal average of σ^0_{HH} did not show clear changes after deforestation events, but the temporal average of σ^0_{HV} was systematically decreased 3-5 dB after deforestation events.

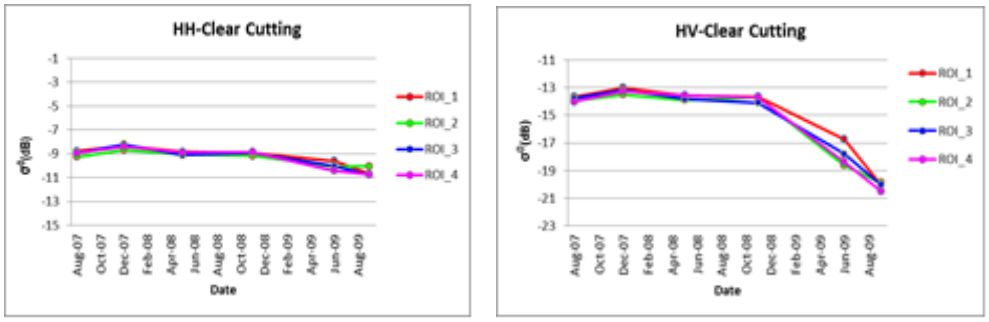

(a) (b)

Fig 4. Characteristic of backscatter value (σ^0) for HH polarization (a) and HV polarization (b) during deforestation events, (ROI: Region of Interest)

Figure 5 shows the detection rate, false alarm rate, and accuracy rate of deforestation detection obtained by using various thresholds for HH and HV polarization. The false alarm rate of both polarization showed similar behavior and rapidly increased at a threshold around -2 dB and the detection rate rapidly increased at a threshold around – 5 for HH and -7 for HV. The accuracy rate of deforestation detection for HH was significantly smaller than HV polarization. The maximum accuracy rate of HH and HV were 77% and 94.8% respectively when threshold values are -1and -2.5 dB, respectively.

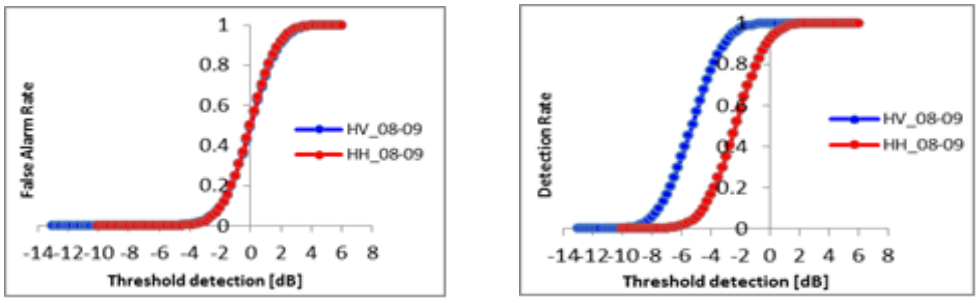

(a) (b)

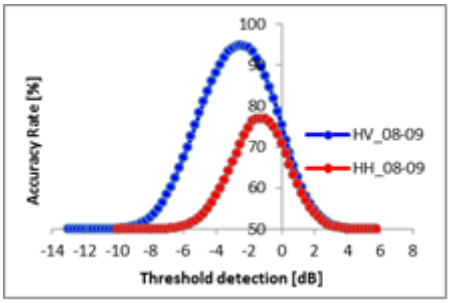

(c)

Fig 5. (a) False alarm rate, (b) detection rate and, (c) accuracy rate for HH and HV polarization

Figure 6 shows the histogram of difference σ^0 for deforested and forest no change areas. For HH polarization image, the number of pixels overlap between deforested and forest no change has been larger than HV polarization image. The error area in HV polarization was very small and the error area in HH polarization was very large. Therefore, HV polarization images became easier to detect the deforested areas from natural forest areas than HH polarization image.

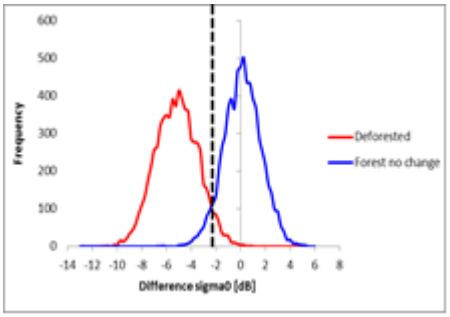

(a)

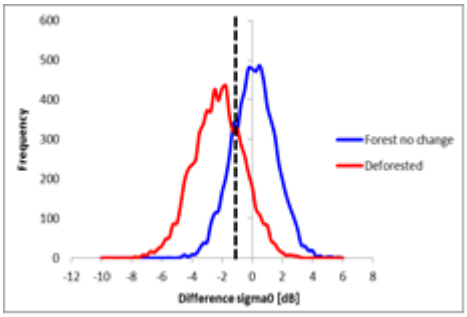

(b)

Fig 6. Histograms of difference σ0 for deforested and forest no change areas, (a) HV polarization, (b) HH polarization

Capabilities of HV polarization on deforestation detection mapping is caused by sensitivity of this signal to vertical objects such as tree trunk. Therefore, the σ^0_{HV} intensity will abruptly decrease after cutting the trees due to changes in scattering mechanism. Decrease in σ^0_{HV} also caused by forest canopies tend to depolarize the radar signal (random scattering: volume scattering), giving a strong HV signal that is lost when deforestation occur.

3.2 The seasonal variation due to moisture effect on radar backscattering coefficient (σ^0)

Figure 7 shows the mean of σ^0_{HV} values of bare soil on wet seasons was larger than dry seasons in both of locations. The other land covers (settlement, forest, acacia and oil palm) were showed no significant change during wet and dry season. The low differences were in settlement and forest. In high accumulated rainfall, σ^0_{HV} values was increased significantly and decreased when the accumulated rainfall in the lowest intensity, especially for bare soil.

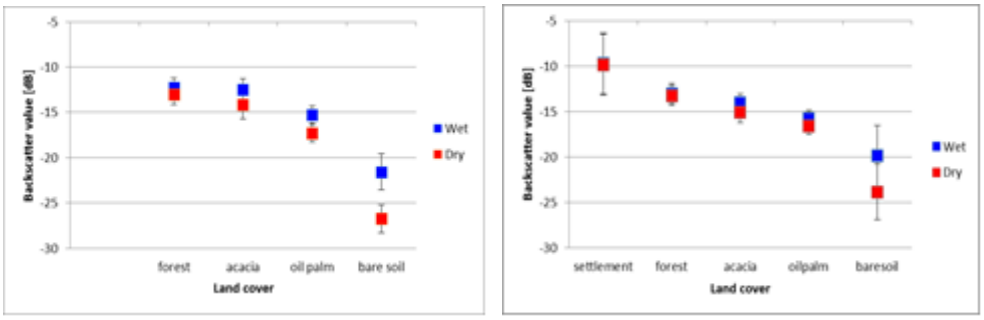

(a) (b)

Fig 7. Seasonally averaged σ^0HV values for each land cover (a) in Borneo and (b) Riau

Analysis of correlation was performed to investigate the correlation between σ^0_{HV} intensity and accumulated rainfall for vegetation and bare soil.

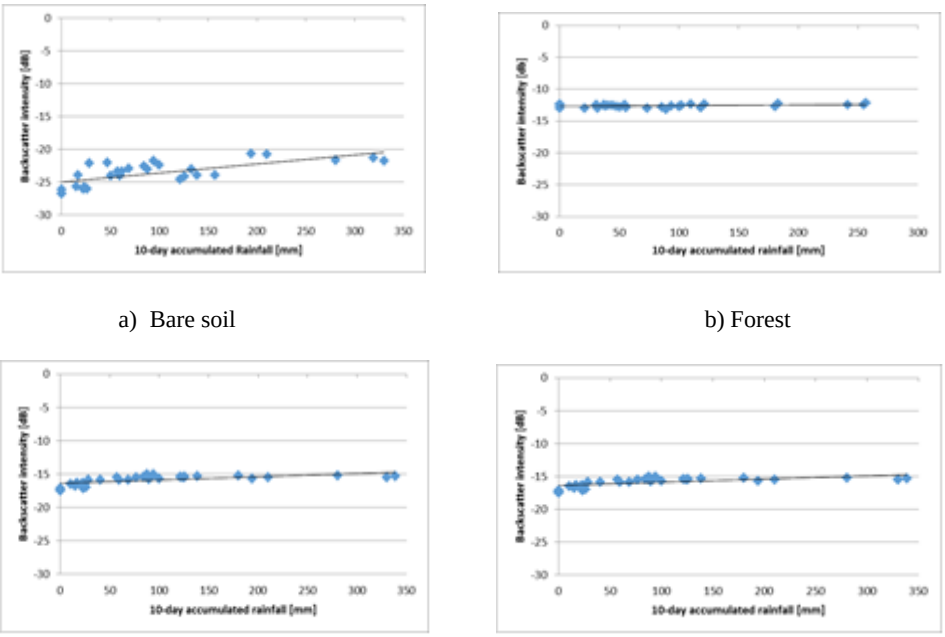

a) Bare soil b) Forest

c) Acacia d) Oil palm

Fig 8. Correlation between backscatter intensity and accumulated rainfall for each land cover

According to Figure 8, coefficient of correlation for forest was lowest among all of the vegetation classes (R= 0.374). The highest coefficient of determination was in bare soil (R= 0.702). The coefficient correlation of acacia and oil palm were 0.631 and 0.639.

The result shows that bare soil has the highest different in dry and wet seasons and positive correlation between σ^0_{HV} of bare soil (deforested areas) and accumulated rainfall. This phenomena caused by the amount of radar energy returned to the antenna (backscattering signal) is depends on the dielectric constant of the target. Heavy rainfall increased soil water content up to 85% at soil depths of 0-40 m (Xiu et al., 2011). Increasing the water content of targets will increase the dielectric constant. Based on radar equation, the dielectric constant is proportional to the backscattering value. Otherwise, at

low concentration of water, most of the molecules bind to the grains, enabling the wave to penetrate into the soil, then reduced the backscattering value.

3.3 Evaluation of seasonal variations effect on deforestation detection

Figure 9 shows the σ^0_{HV} difference between deforested areas and natural forests varied with time using FBD-1. The σ^0_{HV} differences between deforested areas and natural forest sometimes became small as shown in the images acquired in September and October 2009. According to the rainfall data from GsMap, these images acquisition time is coincides with the high accumulated rainfall (>90 mm/10-day).

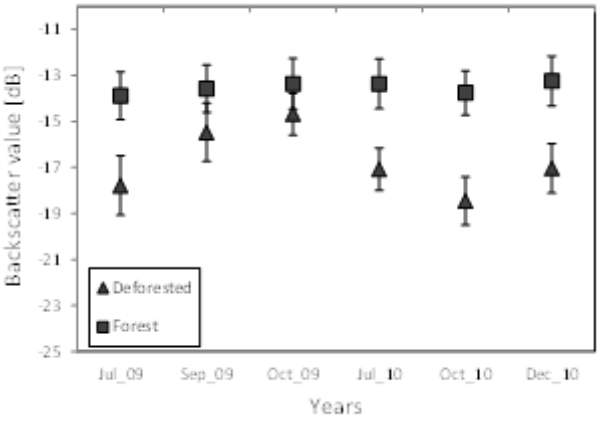

Fig 9. Time series of σ0HV value for natural forest and deforested areas by using FBD-1 data

Figure 10 shows the detection rate, false alarm rate, and accuracy rate of deforestation detection obtained by using various thresholds for the different observation time of σ^0HV. The relationship between the detection rate and thresholds was not always similar and it changed depending on the observation time. The detection rate is rapidly increased at threshold around -8 to -5 dB.

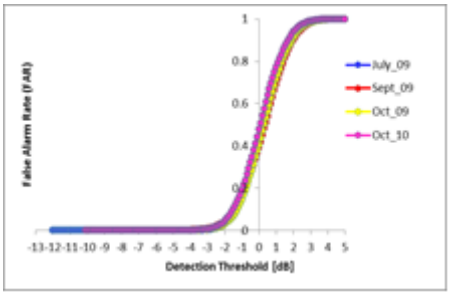

(a)

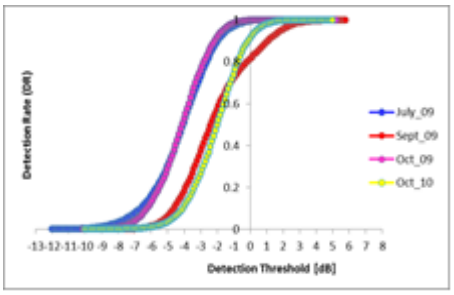

(b)

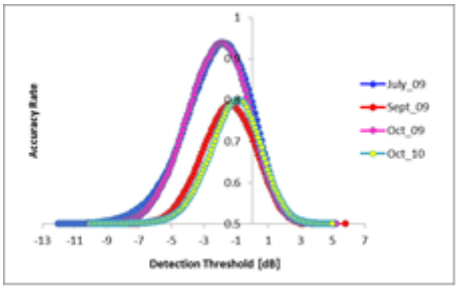

(c)

Fig 10. (a) False alarm rate, (b) detection rate, and (c) accuracy rate of FBD-1 image with different observation time

On the other hand, the false alarm rate for all data showed similar behavior and rapidly increased at a threshold of around -2.0 ~ -1.0 dB. The accuracy rate showed the maximum value when the threshold of the σ^0 difference was between -2 dB and -1dB. The maximum accuracy rate, ranged from 79.05% to 93.84%. The maximum accuracy rate tended to decrease when the σ^0HV differences between deforested areas and natural forest were small as shown in Figure 9.

Figure 11 shows the histogram of difference σ0 for deforested and forest no change areas. For image difference at Nov/07-Oct/09, which has small difference σ^0 in Figure 9 shows that the numbers of pixels overlap between deforested and forests no change is larger than image difference at Nov/07-Oct/10, which has the large difference of σ^0. The error area of difference image at Nov/07-Oct/09 was very small and the error area at Nov/07-Oct/09 was very large. Therefore, image difference that has the large difference of σ0 between deforested and forest no change areas became easier to detect the deforested areas from natural forest areas than the image that has the small difference of σ^0.

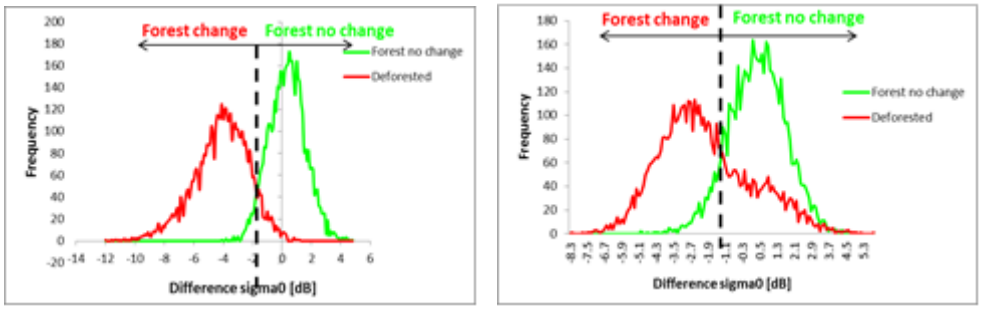

(a) (b)

Fig 11. Histogram of difference σ^0 for natural forest and deforested areas, (a) Image of Nov/07-Oct/10 and (b) Image of Nov/07-Oct/09

Based on data from Table 1, only two images have the better accuracy rate (Nov_07-July_09 and Nov_07-October_10). Therefore, these images were chosen to make the deforestation map of 2009 to 2010.

The positive correlation between σ^0_{HV} of bare soil (deforested areas) and accumulated rainfall can affect the accuracy rate of deforestation detection. In the high-accumulated rainfall, the value of σ^0_{HV} for deforested areas increases and sometimes overlaps with the value of σ^0_{HV} for natural forest. Therefore, the difference σ^0_{HV} value between deforested areas and natural forest become small and the accuracy rate of deforestation detection is decreased. In the low accumulated rainfall, the σ^0_{HV} value of deforested areas was

decreased significantly and the σ^0_{HV} value of natural forest is constant. Therefore, the difference σ^0_{HV} between deforested areas and natural forest become large, so the deforested areas and natural forest is easy to distinguish. In this research, images observation time was selected in dry season to reduce the error in the interpretation of deforestation detection.

Table 1. Accuracy rate of deforestation detection mapping using threshold in FBD-1

Accumulated precipitation (mm/10-day)	Image difference	Maximum Accuracy Rate (%)	Threshold(dB)
0-89	Nov_07-Jul_09	93.76	-1.8
90≤	Nov_07-Sep_09	79.05	-1.3
90≤	Nov_07-Oct_09	79.94	-0.8
0-89	Nov_07-Oct_10	93.84	-1.8

3.4 Deforestation mapping

Figure 12 shows the deforestation map in Riau Province with data period from November 2007 until October 2010 using HV polarization images and maximum threshold (-1.8 dB) based on the results described above. Deforestation areas from November 2007 to July 2009 marked as red color, and July 2009 to October 2010 marked as yellow color. The remaining forest cover area in October 2010 was marked in green color.

Table 2 shows the accuracy of the annual deforestation map assessed by using reference data from Global Forest Watch and land use/cover map from Indonesian Ministry of Forestry. The total pixels of true are 438 pixels and overall accuracy of the mapping was 92.21%, which was almost the same as the accuracy rate obtained in the above-mentioned threshold evaluation.

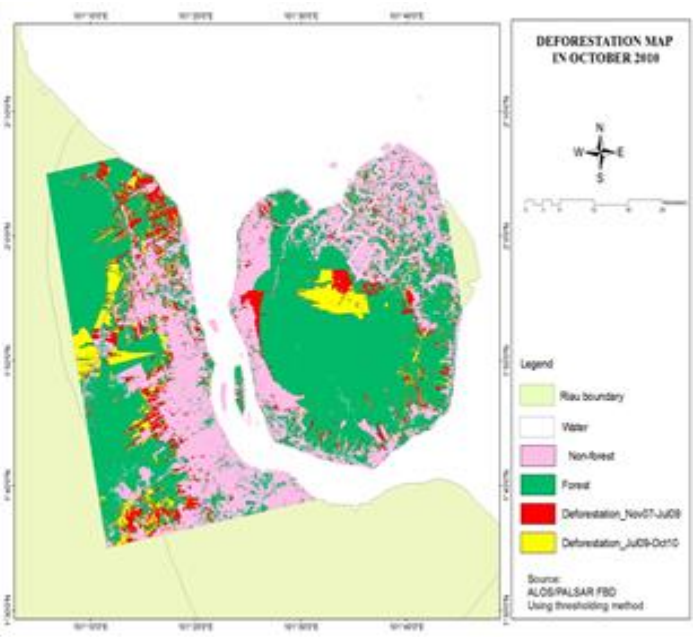

Fig 12. Deforestation map of Riau Province from November 2007 to October 2010

The high accuracy of deforestation detection mapping using ALOS/PALSAR images caused by several factor such as the finer of spatial resolution ALOS/PALSAR data is 12.5m x 12.5 m, the ability of SAR data to provide cloud-free images in tropical forest areas and the sensitivity of multi-polarization SAR data (co and cross- polarization) to detect the deforestation. The L band was representing good classification of vegetation because the L-band has good penetration in vegetation areas.

Table 2. Confusion matrix for the yearly deforestation map obtained from FBD-1 data

		Reference data						User's Accuracy (%)
Detection By ALOS/PALSAR FBD		Water	Forest	Non-forest	Defo 2007-2009	Defo 2009-2010	Total	
	Water	42	0	0	0	1	43	97.67
	Forest	0	57	5	3	5	70	81.43
	Non-forest	3	8	72	2	1	86	83.72
	Defo 2007-2009	0	0	0	153	5	158	96.84
	Defo 2009-2010	0	0	0	4	114	118	96.61
	Total	45	65	77	162	126	475	
Producer's Accuracy (%)		93.33	87.69	93.51	94.44	90.48		92.21

Table 3. Forest covers loss in Riau Province from 2007-2010

Month/Year	Forest cover loss area (ha)	Total Forest cover (ha)	Percentage forest covers loss (%)
Nov/07		182910.712	
N0v/07-Jul/09	15385.34	170525.372	6.77
Jul/09-Oct/10	10371.25	160154.122	6.08

Table 3 shows the total deforested areas calculated by using PALSAR HV polarization data. Based on these data, the total deforested areas from November 2007 to October 2010 were 22756.59 ha. The total forest covers area in November 2007 was182910.712ha. Forest areas in November 2007 reduce to 6.77 % in July 2009 and 6.08 % in October 2010.

The high rate of deforestation in Riau is caused by the clearing of natural forest cover to become non-forest for industrial plantations (pulpwood and oil palm plantation). The WWF 2008 noted that the forest cover lost in the last 25 years is as follows: 24% was replaced by or cleared for industrial pulpwood plantations, 29% was replaced by or cleared for industrial oil palm plantations and 17% became so called "waste land".

4 Conclusion

The accuracy of deforestation detection mapping using HV polarization is giving better results than HH polarization. The better performance of HV polarization on deforestation detection mapping is caused by sensitivity of this signal to vertical objects.

The seasonal changing due to rainfall affected the radar backscattering signatures for bare soil, acacia, and oil palm, but not for forest areas, this phenomena caused by the positive correlation between σ^0_{HV} of bare soil and accumulated rainfall. In addition, high-accumulated precipitation decreased the sigma nought (σ^0) difference between deforested areas and natural forests, causing decreased accuracy of deforestation detection.

The accuracy of deforestation map based on thresholding method is 92.21%. Forest areas in Riau at July 2007 reduce to 6.77 % in July 2009 and 6.08 % in October 2010.

References

1. Hansen, M. C. (2008). Humid tropical forest clearing from 2000 to 2005 quantified by using multi-temporal and multi-resolution remotely sensed data. *Proceedings of the National Academy of Sciences of the United States of America,* 105, pp. 9439–9444.
2. Kiage, L.M., N.D. Walker., S. Balasubramanian, A. Babin., and J. Barras. (2005). Applications of RADARSAT-1 synthetic aperture radar imagery to assess hurricane-related flooding of coastal Louisiana. *International Journal of Remote Sensing,* 26(24), 5359–5380.
3. Margono, B.A., Turubanova, S, Zhuravleva, I, Potapov, P, Tyukavina, A, Baccini, A. (2012). Mapping and monitoring deforestation and forest degradation in Sumatra (Indonesia) using Landsat time series data sets from 1990 to 2010. Environmental

Research Letters,7,034010.http://dx.doi.org/10.1088/1748-9326/7/3/034010 (April 10th 2014).
4. Motohka, T., Shimada, M., Uryu, Y., Setiabudi, B. (2014). Using time series PALSAR gamma naught mosaics for automatic detection of tropical deforestation: A test study in Riau, Indonesia. *Journal Remote Sensing of Environment*. xxx, xxx-xxx.
5. Salas,W. A., Ducey, M. J., Rignot, E, & Skole, D. (2002). Assessment of JERS-1 SAR for monitoring secondary vegetation in Amazonia: I. Spatial and temporal variability in backscatter across a chrono-sequence of secondary vegetation stands in Rondonia. *International Journal of Remote Sensing*, 23, 1357–1379.
6. Shimada, M. (2009). Palsar radiometric calibration and geometric calibration. *IEE Transactions on Geoscience and Remote Sensing*. 47 : 3915 - 3932.
7. Thiel, C.P., Drezet, C. Weise, S. Quegan, & C. Schmullius. (2006). Radar remote sensing for the delineation of forest cover maps and the detection of deforestation. *Journal of Forestry*, 79, 589–597.
8. Tsuyuki, S., How Goh, M., Teo, S., Kamlun, KU. (2011). Monitoring deforestation in Sarawak, Malaysia using multi-temporal Landsat data. University of Malaysia Sabah. https://www.google.co.jp/url?sa=t&rct=j&q=&esrc=s&source=web&cd=1&ved=0CB4QFjAA&url=https%3A%2F%2Fwww.apn-gcr.org%2Fresources%2Farchive%2Ffiles%2Fceaa0b40b089ad8e671c2e79890a6f03.pdf&ei=CQzVKXUDcq2uAT_toLYDg&usg=AFQjCNFzaW20FabSQKO7MnIGVlQOqYU_VA (May 4th 2014)
9. Whittle, M., Quegan, S., Uryu, Y., Stüewe, M., & Yulianto, K. (2012). Detection of tropical deforestation using ALOS-PALSAR: A Sumatran case study. *Remote Sensing of Environment*, 124, 83–98.
10. WWF Indonesia. (2009). Deforestation Forest Degradation Biodiversity Loss and CO2 Emissions in Riau Sumatra Indonesia. Jakarta: WWF Indonesia. https://www.google.co.jp/url?sa=t&rct=j&q=&esrc=s&source=web&cd=1&ved=0CCMQFjAA&url=http%3A%2F%2Fassets.panda.org%2Fdownloads%2Friau_co2_report__wwf_id_27feb08_en_lr_.pdf&ei=3-MzVOeqN5SauQSsoDgDA&usg=AFQjCNFt5kx_rJf_03NDnym8TdAfkXMRfQ (April 9th 2014).
11. Xiu, Q., Liu, S., Wan, X., Jiang, C., Song, X.,Wang, J. (2012). Effect of rainfall on soil moisture and water movement in a subalpine dark coniferous forest in south western China. *Journal of Hydrological Processes*, 26, 3800-3809.